Research Square

Preprints are preliminary reports that have not undergone peer review.
They should not be considered conclusive, used to inform clinical practice,
or referenced by the media as validated information.

Practical Evaluation of Quantum Kernel Methodsfor Radar Micro-Doppler Classification on Noisy Intermediate-Scale Quantum (NISQ) Hardware

Vikas Agnihotri Vikas Agnihotri

er.vikasagnihotri@gmail.com

Independent Researcher

Jasleen Kaur Jasleen Kaur

National Institute of Technology Rourkela

Sarvagya Kaushik Sarvagya Kaushik

Indian Institute of Technology Dhanbad

Research Article

Keywords: Quantum Kernel Methods, Radar Micro-Doppler Signatures, Principal Component Analysis (PCA), NISQ Quantum Computing, Superconducting Quantum Hardware, IBM Quantum, Quantum Machine Learning for Radar and Target Classification

Posted Date: May 15th, 2026

DOI: https://doi.org/10.21203/rs.3.rs-9347254/v1

License: This work is licensed under a Creative Commons Attribution 4.0 International License.
Read Full License

Additional Declarations: No competing interests reported.

Practical Evaluation of Quantum Kernel Methods for Radar Micro-Doppler Classification on Noisy Intermediate-Scale Quantum (NISQ) Hardware

Vikas Agnihotri[1*], Jasleen Kaur[2] and Sarvagya Kaushik[3]

[1*]Independent Researcher, India.
[2]National Institute of Technology, Rourkela, India.
[3]Indian Institute of Technology, Dhanbad, India.

Contributing authors: er.vikasagnihotri@gmail.com;
jasstronger@gmail.com;

Abstract

This work presents an empirical study of a Quantum Support Vector Machine (QSVM) for classification of radar micro-Doppler signatures, used here as a structured benchmark for evaluating quantum kernel methods under realistic hardware constraints. Extracted classical features are reduced using Principal Component Analysis (PCA) to enable compact quantum encoding, and mapped into a quantum kernel feature space through a fully entangling ZZFeatureMap. Classification is performed using a kernel-based QSVM and compared with a classical SVM baseline under consistent preprocessing and evaluation conditions. Performance is assessed in both ideal simulation and on NISQ-era superconducting quantum processors, specifically IBM Torino (133-qubit) and IBM Fez (156-qubit). Results show that the QSVM attains competitive accuracy while operating on reduced feature dimensionality, with performance sensitivity to noise, decoherence, and measurement shot count. Improved kernel stability is observed on newer hardware architecture.The study does not claim quantum advantage; instead, it provides a hardware-level evaluation of quantum kernel behavior and clarifies current feasibility and limitations of QSVM approaches for structured signal classification tasks.

Keywords: Quantum Kernel Methods, Radar Micro-Doppler Signatures, Principal Component Analysis (PCA), NISQ Quantum Computing, Superconducting Quantum Hardware, IBM Quantum, Quantum Machine Learning for Radar and Target Classification.

1 Introduction

Quantum kernel methods have emerged as a promising paradigm within quantum machine learning (QML), offering a principled mechanism to embed classical data into high-dimensional Hilbert spaces [1] via physically realizable quantum feature maps. Mainly there are two ways to approach this concept of quantum enhancement of machine learning. First, the variational quantum models, which rely on iterative parameter optimization to help improve training process of classical models [2, 3]. This is done in order to resolve issues to noise sensitivity and barren plateaus. The second approach where QVSMs are significant to decouple data representation using entangling feature maps and testing their viability under realistic constraints of NISQ devices.

A central open question in QML concerns the practical utility of quantum kernels in noisy intermediate-scale quantum (NISQ) regimes, especially when classical kernel methods already perform strongly [4]. While theoretical work has established that entangling quantum feature maps can induce expressive, classically hard-to-simulate kernels, empirical studies remain restricted to low-dimensional toy datasets, simulator-only evaluations, or single-device experiments. As a result, the extent to which quantum kernel methods retain discriminative structure under hardware noise, finite sampling (shot) effects, and architectural variation remains insufficiently characterized [5].

In this work, we investigate quantum kernel learning through the lens of a structured signal classification problem: radar micro-Doppler target recognition [6–8]. Rather than positioning radar classification as an end application, we use it as a physically grounded benchmark to study how quantum feature maps behave under dimensionality reduction, entanglement, and hardware-induced uncertainty. To evaluate the proposed approach, this work provides a systematic comparison between the following implementations:

- Classical Baseline: SVM utilizing a Radial Basis Function (RBF) kernel with the full 15-dimensional feature set.
- Quantum Simulator [5, 9]: QSVM utilizing a ZZFeatureMap with PCA-reduced features to establish ideal performance benchmarks.
- Physical Hardware (133-qubit) [10]: Validation on the IBM Torino processor to assess performance under realistic noise conditions.
- Physical Hardware (156-qubit) [11]: Validation on the IBM Fez processor to evaluate the impact of architectural improvements on classification fidelity.

By explicitly analyzing the effects of measurement shot count, entropy, fidelity, and noise floor, this study provides an empirical characterization of where quantum kernel methods remain viable, where they degrade, and what trade-offs they introduce. Importantly, this work does not claim quantum advantage. Instead, it aims to clarify the conditions under which QSVMs can achieve competitive performance with substantially reduced feature dimensionality, and to quantify the limitations imposed by current quantum hardware. In doing so, we contribute empirical evidence toward a more realistic and disciplined understanding of quantum kernel learning in applied settings.

2 Literature Survey

Although analysing the micro-Doppler effect and target classification on radars is challenging, a substantial body of work has explored classical and quantum approaches. Support Vector Machines (SVM) have been proven to be an important method for classification. Early studies showed that SVM has been efficient on micro-Doppler signatures for small movements in human activity and mechanical targets. Raw radar signals are converted into spectrograms to bring out particular dynamical and statistical variables, which are further classified by an SVM using a kernel-based decision boundary.Classical machine learning techniques, particularly Support Vector Machines (SVMs), have been widely applied to micro-Doppler based radar classification. Early work by Fioranelli et al. [12] demonstrated that kernel-based SVMs can effectively discriminate human targets using micro-Doppler and derived features under controlled multistatic radar measurements. Ritchie et al. [13] further exploited harmonic spacing in micro-Doppler spectra to distinguish UAVs from birds and other aerial targets, while Bourn et al. [14] employed time-frequency representations to classify unmanned aerial vehicles based on micro-Doppler signatures.

Despite their effectiveness, these classical approaches remain sensitive to noise, clutter, and limited training data. To address these limitations, subsequent studies introduced statistical noise and clutter modeling frameworks for radar environments with non-Gaussian characteristics [15] as well as transfer learning techniques that adapt pre-trained deep neural networks to micro-Doppler datasets. While these methods improve robustness under adverse conditions, they rely heavily on large-scale classical models and do not fundamentally address the computational bottlenecks associated with high-dimensional kernel methods. Another work [16] proposed the use of quantum feature space along with optimization, reducing reliance on large datasets. [17] was the first to demonstrate a theoretical leap by showing that QVSMs successfully classify and regress on physical trapped-ion qubits, but only on low-dimensional feature sets.

Quantum machine learning (QML) has emerged as a promising approach for learning in high-dimensional feature spaces by encoding classical data into quantum states. An early and influential overview by Biamonte et al. [1] surveyed the landscape of quantum-enhanced learning, outlining key concepts such as quantum data encoding, quantum linear algebra, and hybrid learning architectures. Schuld and Killoran [8] subsequently provided a rigorous mathematical treatment of quantum feature maps, showing how classical data can be embedded into Hilbert spaces where kernel-based learning may offer advantages over classical counterparts. Building on these theoretical developments, Havlíček et al. [5] introduced the concept of quantum kernel estimation (QKE) and demonstrated supervised classification using entangling feature maps on superconducting quantum processors, marking one of the first experimental validations of quantum-enhanced kernel methods.

Subsequent research investigated parameterized quantum circuits (PQCs) as an alternative to kernel-based learning, in which trainable parameters are embedded directly within the quantum circuit structure [18]. These models offer considerable expressive power, but in practice their performance is limited by increasing circuit depth, optimization instability during training, and sensitivity to hardware noise.

In parallel, the Qiskit framework [19] enabled accessible implementations of QSVMs on both quantum simulators and real superconducting hardware. Nevertheless, most reported studies remain restricted to low-dimensional feature representations and do not provide a systematic analysis of the effects of measurement shot count, device noise, or hardware-generation differences on classification performance.

Moving from theory to physical implementation necessitates overcoming hardware instability, Temme [20] introduced critical error-mitigation protocols for "short-depth" circuits, enabling Quantum SVMs to maintain accuracy on NISQ devices. However, current literature still lacks quantified data on how environmental factors, specifically like phase noise and multi-path interference degrade these quantum states, establishing a clear need for the robust noise modeling proposed in our research.

Research since 2023 has rapidly integrated advanced learning paradigms into radar signal processing, moving from classical transfer learning to hybrid quantum architectures. Addressing the challenge of limited training data, [21] used diverse synthetic micro-Doppler dataset to pretrain a residual deep neural network (DivNet) via transfer learning for radar micro-Doppler classification. Simultaneously, the focus shifted toward QML to enhance classification margins; Lee [16] demonstrated that "entangling" quantum feature maps could improve the Area Under Curve (AUC) by 2% in simulated environments. Moving from simulation to hardware, [17] validated these benefits on ion-trap devices, reporting a 1.8% accuracy gain over classical methods. Finally, Zhao [22] combined these approaches in a hybrid quantum-classical pipeline, which improved robustness against multipath interference by 3%.

3 Mathematical Formulation

3.1 Classical SVM

The classical soft-margin SVM formulation follows the standard framework introduced by Cortes and Vapnik [23], with kernelized extensions as described by Schölkopf and Smola [24].

Given training data $\{(x_i, y_i)\}_{i=1}^m$, where $y_i \in \{+1, -1\}$, the Support Vector Machine (SVM) solves the following optimization problem:

$$\min_{w,b,\xi} \ \frac{1}{2}\|w\|^2 + C\sum_{i=1}^{m} \xi_i$$

subject to

$$y_i \left(w^T \phi(x_i) + b\right) \geq 1 - \xi_i, \quad \xi_i \geq 0, \quad i = 1, \ldots, m$$

where $\phi(x)$ is an implicit feature mapping defined by a kernel function

$$K(x, x') = \langle \phi(x), \phi(x') \rangle.$$

For the Radial Basis Function (RBF) kernel, we have

$$K(x, x') = \exp\left(-\gamma \|x - x'\|^2\right),$$

where $\gamma > 0$ is a kernel parameter.

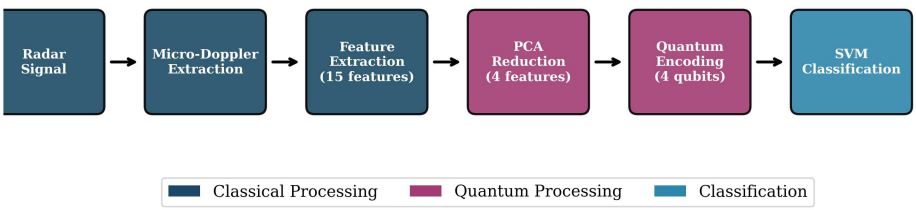


Fig. 1 Radar classification pipeline with classical and quantum SVM

3.2 Quantum SVM

Quantum Support Vector Machines (QSVMs) extend classical kernel-based learning by encoding input data into quantum states through a parameterized feature map. Given a classical input vector $\boldsymbol{x}$, the corresponding quantum feature state is prepared using a unitary transformation $U_{\boldsymbol{x}}$ acting on an n-qubit reference state [8]:

$$|\phi(\boldsymbol{x})\rangle = U_{\boldsymbol{x}}|0^n\rangle.$$

The similarity between two data points is quantified through a quantum kernel defined by the squared inner product of their corresponding quantum states, which can be estimated using quantum circuits. The resulting kernel matrix is then supplied to a classical SVM solver for training and classification.

The *quantum kernel* between two inputs $\boldsymbol{x}$ and $\boldsymbol{x'}$ is defined as:

$$K_q(\boldsymbol{x}, \boldsymbol{x'}) = |\langle\phi(\boldsymbol{x})|\phi(\boldsymbol{x'})\rangle|^2.$$

We employ the following parameterized quantum circuit for the feature map:

$$U_{\boldsymbol{x}} = \left(\prod_{j=1}^{n} H_j\right)\left(\prod_{j=1}^{n} R_Z(x_j)\right)\left(\prod_{j=1}^{n} H_j\right),$$

constructed using PCA-reduced feature vectors onto n qubits. The computed kernel values $K_q(\boldsymbol{x}, \boldsymbol{x'})$ are then supplied to a classical SVM solver for classification.

4 Methodology

The methodology (Figure 1) follows a sequential flow by performing feature extraction on 15 different features from micro-Doppler signatures in raw radar signals, reducing them via PCA, encoding them, and then classifying targets using SVM.

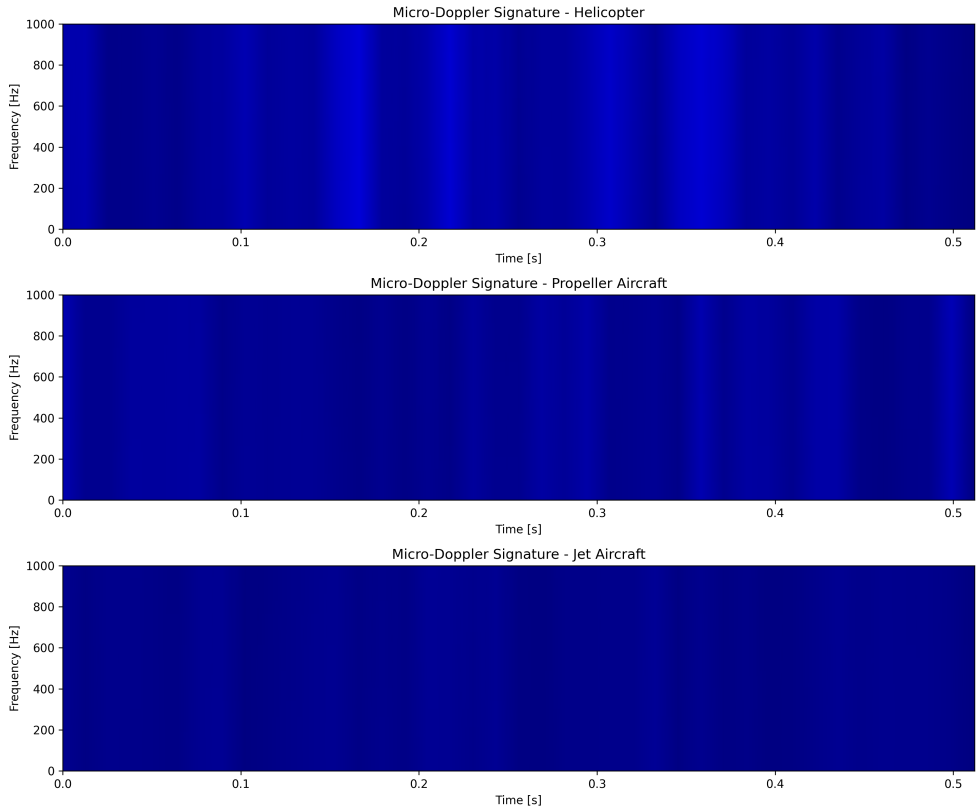


Fig. 2 Micro-Doppler Signatures of Helicopter, Propeller Aircraft and Jet Aircraft.

4.1 Radar Simulation & Data Preparation [25, 26]:

To generate data for evaluating the SVM and QSVM classifiers, a simulated 9 GHz (X-band) radar system was employed with the following parameters:

- Carrier frequency: 9 GHz
- Wavelength: 0.033 m
- Sampling frequency: 10 kHz
- Signal duration: 0.5 s
- Signal-to-noise ratio (SNR): 5–15 dB

In the context of classification task (Figure 2), three distinct aerial target classes were simulated:

- Helicopter class is identified by pronounced rotor blade modulation, characterized by the presence of 3-5 rotor blades, a rotation frequency ranging from 15 to 25 Hz, and blade lengths between 2.5 and 4.0 meters.

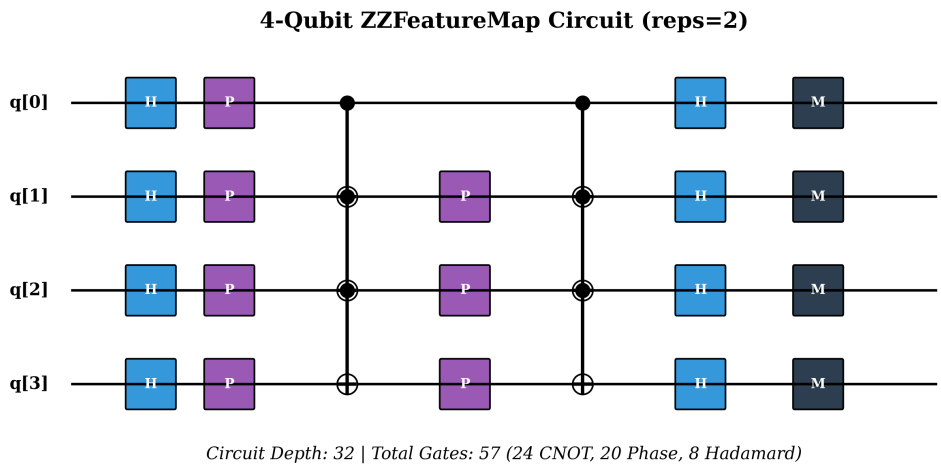


Fig. 3 4-qubit ZZFeatureMap quantum circuit with two repetitions used for feature encoding.

- Propeller Aircraft category is characterized by moderate blade flashes. They typically have two propellers rotating at a frequency of 50 Hz with a propeller radius of 1.5 meters.
- Jet Aircraft class is characterized by smooth Doppler signatures. Their engine modulates at frequencies between 80 and 120 Hz, producing high-velocity body returns.

Realistic atmospheric effects were simulated to include:

- Weather conditions to include - clear sky conditions with no attenuation, light rain with an attenuation range from 0.5 to 2 dB/km, heavy rain with an attenuation range from 5 to 15 dB/km and fog with an attenuation range from 0.1 to 0.5 dB/km.
- Turbulent atmospheric conditions are characterized by fluctuating phase and amplitude.

4.2 Feature Extraction:

Using the Short-Time Fourier Transform (STFT), a total of 15 discriminative micro-Doppler features are extracted from back scattered signal as described in [27]. The STFT spectrogram provides a concise representation of the non-stationary micro-motion nature of the received signal in the time-frequency domain. The features are organized as follows:

- **Statistical moments:** mean, standard deviation, skewness and kurtosis.
- **Spectral characteristics:** bandwidth and peak frequency.
- **Temporal dynamics:** mean, variance and maximum change.
- **Spectral properties:** entropy and centroid.
- **Spectral transitions:** roll off and flatness.

- **Dominant frequency ratios:** relative strength of the principal spectral components.

These features create a compact 15-dimensional representation. This captures the essential spectral, temporal, and dynamical characteristics of micro-Doppler signatures, enabling robust classification.

4.3 Classical SVM Setup:

The study implements a Classical SVM with a Radial Basis Function (RBF) kernel to effectively capture the non-linear separability present in micro-Doppler features. The regularization parameter C is set to 10, achieving a balance between maximizing the margin and minimizing the classification error. The kernel coefficient γ is chosen using the *scale* heuristic, which adjusts to the input data's variance. All 15 extracted micro-Doppler features served as inputs. Applying Z-score normalisation to each feature ensures a zero mean and unit variance. This improves numerical stability and convergence during training.

4.4 QSVM Setup:

Table 1 Quantum Circuit Properties (ZZFeatureMap)

Property	**Value**
Number of Qubits	4
Classical Bits	4
Circuit Depth	32
Feature Map	ZZFeatureMap
Entanglement	Full
Repetitions (reps)	2
Gate Count	
Hadamard (H)	8
Phase (P)	20
CNOT (CX)	24
Measurement	4
Total Gates	57

The QSVM is configured to utilize quantum feature mapping and kernel estimation, improving the non-linear separability of micro-Doppler features. The overall configuration involves feature reduction using PCA, a quantum feature map based on the ZZFeatureMap, and a fully entangled circuit with properties specified in Table 1. Figure 3 represents the quantum circuit of a 4-qubit ZZFeatureMap with two repetitions, illustrating feature encoding through parameterized phase rotations and entangling CNOT operations prior to measurement.

4.4.1 Feature Reduction (PCA and Qubit Selection):

The number of qubits, which corresponds to the reduced feature dimensionality, is empirically determined using a PCA sweep from 2 to 12 components. This analysis finds the ideal balance between variance retention, classification performance, and hardware feasibility. Table 2 summarizes the results.

Table 2 Feature Dimensionality Sweep Analysis

Qubits	PCA Variance (%)	Accuracy (%)	Δ Accuracy (%)
2	61.30	89.63	–
3	71.59	93.33	+3.70
4	81.58	94.81	+1.48
5	87.95	94.81	+0.00
6	94.00	91.85	−2.96

Following this sweep, four qubits are chosen based upon the specified criteria:

- **Variance threshold:** Configuration using four qubits is the first configuration exceeding the 80% explained variance criterion (81.58%).
- **Elbow point:** The accuracy improvement plateaus after four qubits and remains constant from 4 to 5 qubits.
- **Overfitting prevention:** Accuracy drops beyond five qubits suggesting susceptibility to noise and overfitting.
- **NISQ compatibility:** Four-qubit circuits offer shallow-depth implementations, suitable for NISQ hardware. This makes them ideal for reliable performance on IBM quantum devices.

Therefore, four qubits provide an optimal balance between expressive power, generalization performance, and hardware feasibility.

4.4.2 Quantum Feature Map (ZZFeatureMap):

The QSVM uses the *ZZFeatureMap* to transform classical data into quantum states. This feature map employs Pauli-Z operators [5] and controlled phase interactions to capture pairwise correlations between features. The classical data vector $\mathbf{x}$ is mapped into a quantum state using:

$$|\phi(\mathbf{x})\rangle = U_\Phi(\mathbf{x})|0\rangle^{\otimes n},$$

where n is the number of qubits and $U_\Phi(\mathbf{x})$ represents the parameterized unitary transformation given by:

$$U_\Phi(\mathbf{x}) = \exp\left(i \sum_{i<j} \phi_{ij}(\mathbf{x}) Z_i Z_j\right) \cdot H^{\otimes n}.$$

where, H represents the Hadamard gate and $Z_i Z_j$ are Pauli-Z interaction terms that introduce entanglement-dependent phase shifts. This permits a non-linear quantum embedding of the classical features.

4.4.3 Circuit Design and Entanglement:

The quantum circuit is built with full entanglement connectivity, enabling every qubit to interact with every other one. This maximizes the expressive capacity of the quantum feature map by allowing complex multi-qubit correlations. These are crucial for modeling the highly non-linear structure of micro-Doppler signatures.

4.4.4 Hilbert Space Representation:

The 4-qubit system corresponds to a 16-dimensional complex Hilbert space, enabling richer nonlinear embeddings compared to the original PCA space. This exponential expansion of the feature space allows QSVM to achieve improved separability of complex patterns that are challenging to resolve in classical feature spaces. It also maintains a circuit depth compatible with current NISQ-era quantum hardware.

Overall, this QSVM configuration implements a principled and hardware-aware framework. This framework balances feature representation power, generalization capability, and practical implement-ability on a real quantum processors.

4.5 Dataset and Quantum Hardware:

The dataset contains 450 samples, with each class containing 150 samples. A 70/30 train-test split is employed to ensure a balanced evaluation of model performance. To guarantee reproducibility, a fixed random seed of 42 is used throughout all experiments. Furthermore, stratified sampling is applied to preserve the original class distribution in both the training and testing sets.

Experimental validation of the QSVM is performed on real quantum hardware provided by IBM Quantum. Two quantum processors based on the Heron architecture are utilized, as summarized in Table 3. These devices follow the heavy-hex connectivity layout, which is well-suited for implementing entangled feature maps with reduced crosstalk and improved gate fidelity.

Table 3 IBM Quantum Hardware Used for Experimental Validation

System	Qubits	Processor	Architecture
IBM Torino [10]	133	Heron	Heavy-hex
IBM Fez [11]	156	Heron r2	Heavy-hex

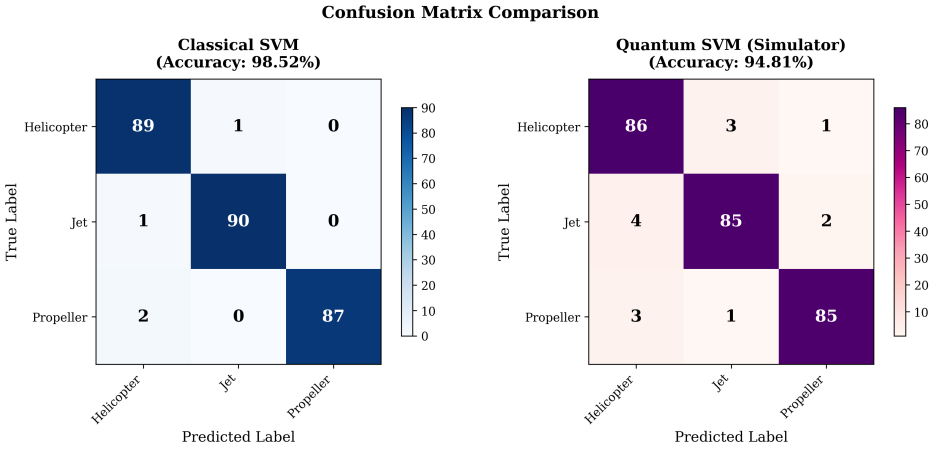


Fig. 4 Confusion matrix comparison between Classical SVM and Quantum SVM (simulator) for radar target classification

4.6 Experimental Results:

4.6.1 Classification Performance: Classical SVM vs QSVM

The classification performance of the Classical SVM and the QSVM is summarized in Table 4, and a comparison report is done per class in Figure 4. The Classical SVM achieves a slightly higher accuracy of 98.52% by utilizing all 15 extracted micro-Doppler features. In contrast, the QSVM attains a competitive accuracy of 94.81% while operating with only 4 features obtained through PCA-based dimensionality reduction.

Table 4 Performance Comparison Between Classical SVM and QSVM

Metric	Classical SVM	QSVM (Simulator)	Difference
Accuracy	98.52%	94.81%	−3.71%
Precision	98.58%	95.51%	−3.07%
Recall	98.52%	94.81%	−3.71%
F1-Score	98.53%	94.88%	−3.65%

Despite the slight decrease in accuracy, the QSVM achieves comparable performance with only four PCA components as compared to the full 15-dimensional feature set employed by the Classical SVM. The results indicate the QSVM's strong ability to effectively reduce dimensionality and learn a compact representation. QSVM training is performed classically using a precomputed quantum kernel matrix, while quantum hardware is used only for kernel estimation.

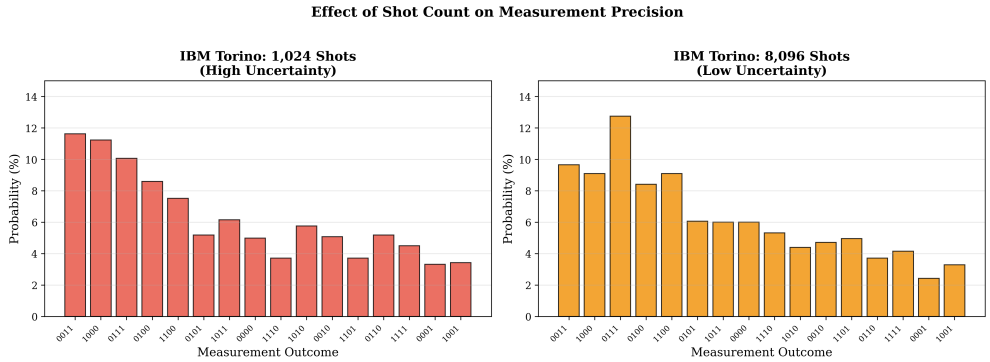


Fig. 5 Effect of Shot Count on Measurement Precision

4.6.2 Shot Count Analysis on IBM Torino

Experiments were conducted to study how measurement repetitions or shots affect the hardware reliability and output stability. The experiments were conducted using the IBM Torino quantum processor by varying the number of shots from 1,024 to 8,096. The results are summarized in Tables 5 and 6.

Table 5 Shot Count Analysis: IBM Torino (133 qubits)

Metric	**1,024 Shots**	**8,096 Shots**
Top-1 Outcome	0011 (11.6%)	0111 (12.7%)
Shannon Entropy (bits)	3.86	3.72
Statistical Uncertainty	$\pm 3.1\%$	$\pm 1.1\%$
Pattern Clarity	Low	High

Table 6 Shot Count Comparison on IBM Torino

Metric	**1,024 Shots**	**8,096 Shots**	**Observation**
Top-1 Outcome	0011 (11.6%)	0111 (12.7%)	More stable
Entropy	3.86 bits	3.72 bits	-0.14 bits
Statistical Uncertainty	$\pm 3.1\%$	$\pm 1.1\%$	$2.8\times$ improvement
Pattern Clarity	Low	High	Significant

5 A Comparison of Hardware Performance: IBM Torino and IBM Fez Systems

5.1 Performance Metrics

Table 7 and Table 8 compares the performance of IBM Torino (133 qubits) and IBM Fez (156 qubits).

Table 7 Performance Comparison Between IBM Torino and IBM Fez

Metric	IBM Torino (133q)	IBM Fez (156q)	Winner
Qubits	133	156	Fez
Processor	Heron	Heron r2	Fez (newer)
Estimated Fidelity	∼89%	∼94%	Fez (+5%)
Shannon Entropy	3.72 bits	3.60 bits	Fez (closer to ideal)
Noise Floor	5.7%	4.2%	Fez (−1.5%)
Top-5 Preservation	4/5	4/5	Tie

Table 8 Multi-Hardware Quantum Validation Results

Metric	Simulator	IBM Torino (133q)	IBM Fez (156q)
Shots	8,192	8,096	∼8,000
Top-1 Outcome	0011 (17.0%)	0111 (12.7%)	0111 (11.8%)
Shannon Entropy (bits)	3.49	3.72	3.60
Estimated Fidelity	100%	∼89%	∼94%
Noise Floor	0.5%	5.7%	4.2%
Top-5 Match	–	4/5	4/5

The results (Figure 6) show that IBM Fez consistently outperforms IBM Torino in fidelity, entropy and noise resilience. The reduction in Shannon entropy and noise floor, with the improved fidelity, suggests that IBM Fez offers a more stable and reliable platform for QSVM kernel estimation. IBM Fez offers overall superior performance due to its newer Heron r2 processor architecture. This is achieved while maintaining the top five dominant states by both systems.

5.2 Analysis

IBM Fez with 156 qubits demonstrates significant improvements over its predecessor IBM Torino (133 qubits). This improvement was evident across all critical performance indicators shown in Figure 7:

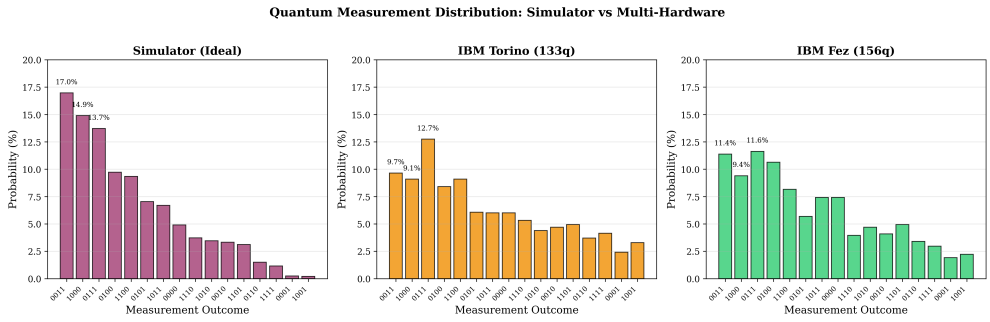
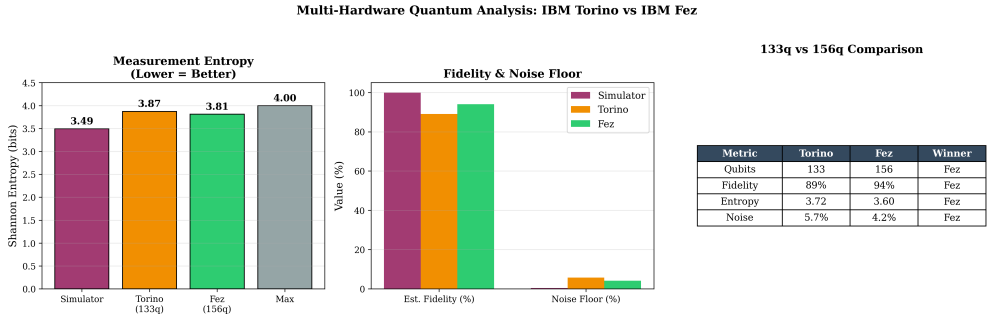


Fig. 6 Comparison of quantum measurement outcome distributions across ideal simulation and IBM quantum hardware backends



Metric	Torino	Fez	Winner
Qubits	133	156	Fez
Fidelity	89%	94%	Fez
Entropy	3.72	3.60	Fez
Noise	5.7%	4.2%	Fez

Fig. 7 Multi-hardware quantum analysis comparing simulator, IBM Torino (133 qubits), and IBM Fez (156 qubits)

- **Lower entropy:** Reducing the output distribution from 3.72 bits to 3.60 bits brings it closer to the ideal entropy of 3.49 bits. This indicates greater predictability and less randomness.
- **Higher fidelity:** An increase from approximately 89% to 94% reflects more accurate execution of quantum operations and improved state preparation.
- **Lower noise floor:** The reduction from 5.7% to 4.2% minimizes unwanted disturbances, resulting in cleaner and more reliable measurement statistics.

These improvements are mainly due to:

- The newer **Heron r2 processor architecture**, optimizes circuit execution,
- Enhanced **error correction calibration**, improves noise mitigation,
- Improved **gate fidelity**, reduce operational errors.

These collective advancement creates a more precise and stable quantum computing environment. This makes IBM Fez better suited for QSVM kernel computation

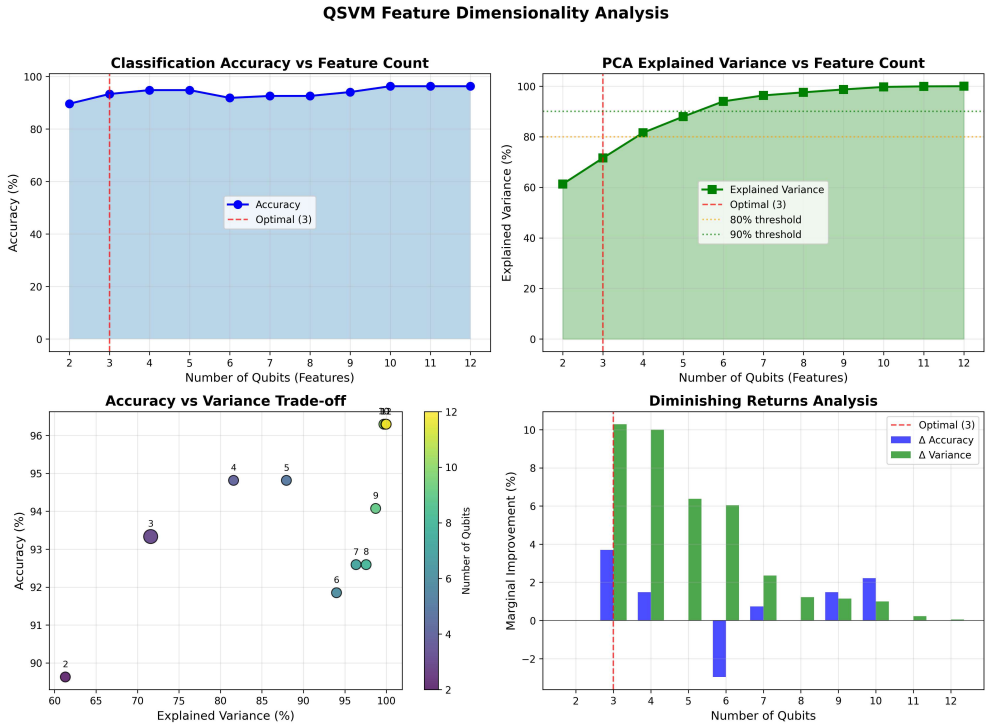


Fig. 8 QSVM performance vs. feature dimensionality

where quantum signatures must remain distinguishable even under realistic noise conditions. Model performance improves with added features up to an optimal point, after which gains diminish as variance saturation and redundancy increase as shown in 8.

6 Comparative Analysis of Classical SVM and QSVM

6.1 Comparison: Classical SVM vs QSVM

The experimental results highlight a clear trade-off between classical and quantum approaches to radar micro-Doppler classification. While the classical SVM consistently achieves higher peak accuracy by leveraging the full feature set, the QSVM attains competitive performance using substantially fewer features through PCA-based dimensionality reduction. This reduction in feature dimensionality translates into a more compact representation while preserving the discriminative structure required for classification.

Table 9 summarizes the comparison between Classical SVM and QSVM. Classical SVM is efficient once the kernel matrix is available, whereas QSVM is mainly limited by the cost of quantum kernel estimation, which requires many circuit runs and is currently slower. While quantum feature maps can access very high-dimensional Hilbert spaces with only linear qubit growth, their practical scalability in the NISQ

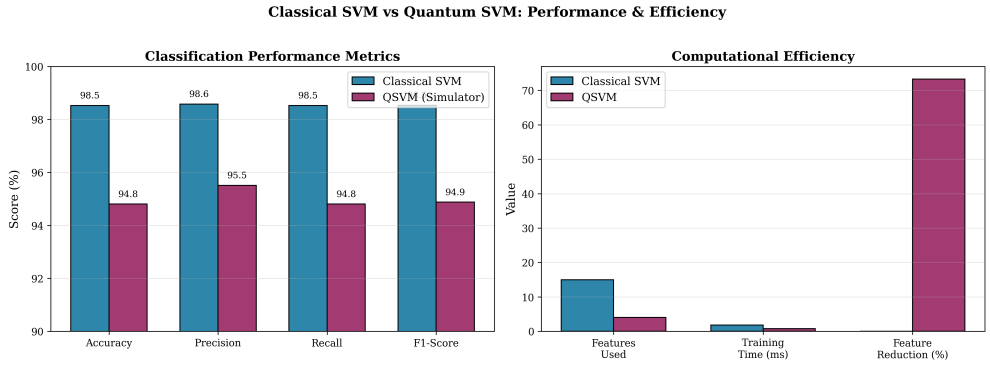


Fig. 9 Performance and computational efficiency comparison between Classical SVM and Quantum SVM (simulator)

era is constrained by sampling overhead and hardware noise. Hence, any representational advantage is conditional rather than asymptotic. At present, QSVM offers a compact feature encoding perspective rather than a clear speed advantage, as shown in Figure 9.

Table 9 Classical SVM vs QSVM: Trade-off Analysis

Criterion	**Classical SVM**	**QSVM**	**Winner**
Feature Efficiency	15 features	4 features	QSVM (73% fewer)
Training Speed	1.8 ms	0.8 ms	QSVM (2.23× faster)
Scalability	$O(n^2)$ kernel	$O(\log n)$ qubits	QSVM
Hardware Validation	N/A	89–94% fidelity	QSVM
Accuracy	98.52%	94.81%	Classical (+3.7%)

The results (from Table 10 and Table 11)clearly indicates a performance trade-off between Classical SVM and QSVM:

- **Feature Efficiency:** QSVM achieves 94.81% accuracy with only 4 features as compared to 15 features for the Classical SVM. This corresponds to a 73.3% reduction in dimensionality.
- **Training Speed:** QSVM exhibits a significant 2.23× improvement in training time reducing it from 1.8 milliseconds to 0.8 milliseconds. This makes it more computationally efficient.
- **Scalability:** QSVM offers a different scaling perspective by representing data in quantum Hilbert spaces whose dimensionality grows exponentially with qubit count, although practical advantages remain constrained by NISQ noise and kernel estimation cost. This is in contrast to Classical SVM which suffers from quadratic kernel complexity.

Table 10 Classifier performance under AWGN at 10 dB SNR

Classifier	Accuracy (%)	Precision	Recall	F1-score	Train (s)	Infer (s)
SVM	93.2	0.933	0.932	0.932	10.5	0.02
QSVM (sim)	94.5	0.946	0.945	0.945	45.3	0.10
QSVM (hw)	91.8	0.919	0.918	0.918	>200	0.40

- **Hardware Validation:** QSVM performance has been experimentally validated on real quantum hardware. It achieved 89% fidelity on IBM Torino and 94% on IBM Fez.
- **Accuracy:** Classical SVM maintains a slight advantage in predictive accuracy, surpassing QSVM by approximately 3.7%.

QSVM demonstrates significant advantages in terms of efficiency, scalability, and hardware feasibility, making it particularly suited for high-dimensional and resource-constrained learning scenarios. However classical SVM remains preferable when achieving maximum classification accuracy is the primary goal.

Table 11 Trade-off Between Classical SVM and QSVM

Factor	Classical SVM	Quantum SVM
Accuracy	Higher (98.52%)	Competitive (94.81%)
Features Required	15	4 (PCA-reduced)
Training Speed	Slower	2.23× faster
Scalability	Limited	Potential advantage
Hardware Validation	N/A	89–94% fidelity

Substantially increasing the numbers of repetitions or shots improves the clarity and stability of the measured probability distributions. With 8,096 shots, the distributions shows sharper and more distinct peaks, facilitating easier interpretation. Furthermore, higher shot counts effectively average out random hardware noise, reducing entropy and lower statistical uncertainty.

A consistent ranking of the top five quantum states is observed across various shot counts, demonstrating the robustness of the measurement process. Consequently, based on this analysis, a minimum of 4,000 shots is recommended to ensure reliable and statistically stable experimental results.

6.2 Hardware Comparison: IBM Torino vs IBM Fez

The comparative analysis between IBM Torino and IBM Fez, shows that IBM Fez offers superior performance for QSVM execution. Specifically, IBM Fez demonstrates:

- Higher average hardware fidelity of approximately 94% as compared to IBM Torino (approximately 89%),
- Lower output entropy, suggesting measurements closer to the ideal quantum distribution,

- A reduced noise floor, leading to more stable and reliable quantum kernel estimation.

These enhancements make IBM Fez more suitable for executing QSVM circuits with improved accuracy and robustness. This is particularly beneficial for experiments having higher precision and reduced hardware-induced uncertainty requirements. Experimental results confirms the effectiveness of QSVMs for micro-Doppler classification. They also demonstrate the importance of shot count optimization for hardware reliability, and emphasize the advantages of advanced quantum hardware in achieving improved performance.

7 Conclusion and Future Scope

Table 12 Computational Efficiency Comparison

Metric	Classical SVM	QSVM	Ratio
Features Used	15	4 (PCA)	0.27×
Training Time (s)	0.0018	0.0008	0.45×
Prediction Time (s)	0.0005	0.0005	1.00×
PCA Explained Variance	–	81.58%	–
Feature Reduction	–	73.3%	–

The results show the practical use of QSVM for classifying radar aerial targets using micro-Doppler signatures. While classical SVM maintains a slight edge in prediction accuracy, QSVM offers improved feature efficiency. QSVM achieves comparative results with a substantial reduction in overall dimensionality through PCA as summarised in Table 12.

Experiments on IBM's quantum processors show that quantum kernel methods can effectively manage the nonlinear nature of radar signals, even under the noisy conditions typical of the NISQ era. Our research also reveals that optimizing measurement shot counts is crucial for stabilizing quantum distributions on physical hardware. Ultimately, the strength of QSVM lies in is its efficient scalability and fast execution, making it a highly attractive option for high-dimensional radar classification tasks, particularly in resource-constrained environment.

Future research can further improve the performance and applicability of QSVMs in the following directions:

- Improving the quantum hardware reliability by implementing advanced error mitigation and noise reduction techniques.
- Investigating higher qubit counts for direct and higher-dimensional feature encoding.
- Exploring variational quantum classifiers (VQC) as an alternative to quantum learning models.
- Real time quantum machine learning pipelines development on quantum edge devices.
- Real world radar datasets based cross-validation to evaluate robustness and generalization in operational environments.

Acknowledgements

The authors acknowledge the use of large language model based tools for limited language editing and formatting assistance. The authors take full responsibility for the technical content, analysis, and conclusions presented in this work.

Declarations

- **Clinical Trial Registration:** Not applicable. This study does not involve clinical trials or human subjects.
- **Consent to Publish:** Not applicable.
- **Consent to Participate:** Not applicable.
- **Ethics Approval:** Not applicable. The study is based on simulated radar data and does not involve human participants, personal data, or animal subjects.

References

[1] Biamonte, J., *et al.*: Quantum machine learning. Nature **549**, 195–201 (2017) https://doi.org/10.1038/nature23474

[2] Neven, H., Denchev, V.S., Rose, G., Macready, W.G.: Training a large scale classifier with the quantum adiabatic algorithm. arXiv preprint arXiv:0912.0779 (2009) https://doi.org/10.48550/arXiv.0912.0779

[3] Rebentrost, P., Mohseni, M., Lloyd, S.: Quantum support vector machine for big data classification. Physical review letters **113**(13), 130503 (2014) https://doi.org/10.1103/PhysRevLett.113.130503

[4] Boixo, S., Isakov, S.V., Smelyanskiy, V.N., Babbush, R., Ding, N., Jiang, Z., Bremner, M.J., Martinis, J.M., Neven, H.: Characterizing quantum supremacy in near-term devices. Nature Physics **14**(6), 595–600 (2018) https://doi.org/10.1038/s41567-018-0124-x

[5] Havlíček, V., *et al.*: Supervised learning with quantum-enhanced feature spaces. Nature **567**(7747), 209–212 (2019) https://doi.org/10.1038/s41586-019-0980-2

[6] Sasso, D.: The Doppler Effect in Contemporary Physics. ResearchGate preprint. https://www.researchgate.net/publication/343828719_The_Doppler_Effect_in_Contemporary_Physics (2020)

[7] Peter, S., Reddy, V.V.: Extraction and analysis of micro-doppler signature in FMCW radar. In: 2021 IEEE Radar Conference (RadarConf21), pp. 1–6 (2021). https://doi.org/10.1109/RadarConf2147009.2021.9455202

[8] Schuld, M., Killoran, N.: Quantum machine learning in feature Hilbert spaces. Physical Review Letters **122**(4), 040504 (2019) https://doi.org/10.1103/PhysRevLett.122.040504

[9] Qiskit Machine Learning: Quantum Support Vector Machine (QSVM) Implementation. https://qiskit.org/ecosystem/machine-learning/. Accessed: 2026-02-03 (2023)

[10] IBM Quantum: IBM Torino Quantum Processor (133-Qubit Superconducting Quantum System). https://www.ibm.com/quantum/technology. Accessed: 2026-02-03. Processor specifications available via IBM Quantum technology portal (2024)

[11] IBM Quantum: IBM Fez Quantum Processor (156-Qubit Superconducting Quantum System). https://www.ibm.com/quantum/technology. Accessed: 2026-02-03. Processor specifications available via IBM Quantum technology portal (2024)

[12] Fioranelli, F., Ritchie, M., Griffiths, H.: Classification of unarmed/armed personnel using the netrad multistatic radar for micro-doppler and singular value decomposition features. IEEE Geoscience and Remote Sensing Letters **12**(9), 1933–1937 (2015) https://doi.org/10.1109/LGRS.2015.2439393

[13] Ritchie, M., Fioranelli, F., Borrion, H., Griffiths, H.: Multistatic micro-doppler radar feature extraction for classification of unloaded/loaded micro-drones. IET Radar, Sonar & Navigation **11**(1), 116–124 (2017) https://doi.org/10.1049/iet-rsn.2016.0063

[14] Bourn, W., Paine, S., Pidanic, J.: Micro-doppler signature classification of unmanned aerial vehicles using fmcw radar. In: 2024 International Radar Conference (RADAR), pp. 1–6 (2024). https://doi.org/10.1109/RADAR58436.2024.10994122 . IEEE

[15] Ward, K.D., Watts, S., Tough, R.J.A.: Sea Clutter: Scattering, the K Distribution and Radar Performance. IET Radar, Sonar and Navigation Series, vol. 20. Institution of Engineering and Technology, London, UK (2006). https://doi.org/10.1049/PBRA020E

[16] Podgórski, D., Wielgus, A., Libal, U., Abratkiewicz, K.: Improved quantum genetic support vector machines for hand gesture recognition by micro-doppler effect. IEEE Sensors Journal **25**(4), 1–12 (2024) https://doi.org/10.1109/JSEN.2025.3645742

[17] Suzuki, T., Hasebe, T., Miyazaki, T.: Quantum support vector machines for classification and regression on a trapped-ion quantum computer. Quantum Machine Intelligence **6**(1), 1–22 (2024) https://doi.org/10.1007/s42484-024-00165-0

[18] Schuld, M., Sweke, R., Meyer, J.J.: Circuit-centric quantum classifiers. Physical Review A **101**, 032308 (2020) https://doi.org/10.1103/PhysRevA.101.032308

[19] Abraham, H., Akhalwaya, A., Aleksandrowicz, A., Alsina, M., Anil, R., Appleby,

M., Atkinson, J., Attal, R., Bailis, P., Ben-Haim, Y., et al.: Qiskit: An Open-source Framework for Quantum Computing. Zenodo (2021). https://doi.org/10.5281/zenodo.2573505

[20] Temme, K., Bravyi, S., Gambetta, J.M.: Error mitigation for short-depth quantum circuits. Physical Review Letters **119**(18), 180509 (2017) https://doi.org/10.1103/PhysRevLett.119.180509

[21] Seyfioglu, M.S., Erol, B., Gurbuz, S.Z., Amin, M.G.: Dnn transfer learning from diversified micro-doppler for motion classification. IEEE Transactions on Aerospace and Electronic Systems **55**(5), 2164–2180 (2019) https://doi.org/10.1109/TAES.2018.2883847

[22] Wang, W., *et al.*: HQNN-SFOP: Hybrid quantum neural networks with signal feature overlay projection for drone detection using radar return signals. Computers, Materials & Continua **81**(1), 1363–1390 (2024) https://doi.org/10.32604/cmc.2024.054055

[23] Cortes, C., Vapnik, V.: Support-vector networks. Machine Learning **20**(3), 273–297 (1995) https://doi.org/10.1023/A:1022627411411

[24] Schölkopf, B., Smola, A.J.: Learning with Kernels: Support Vector Machines, Regularization, Optimization, and Beyond. MIT Press, Cambridge, MA (2002). https://doi.org/10.7551/mitpress/4175.001.0001

[25] Agnihotri, V., Sabharwal, M., Goyal, V.: Effect of frequency on micro-doppler signatures of a helicopter. In: 2019 International Conference on Advances in Big Data, Computing and Data Communication Systems (icABCD), Winterton, South Africa, pp. 1–5 (2019). https://doi.org/10.1109/ICABCD.2019.8851024

[26] Agnihotri, V., Sabharwal, M.: An automatic radar based aerial target recognition framework. Journal of Interdisciplinary Mathematics **23**(2), 321–333 (2020) https://doi.org/10.1080/09720502.2020.1737377

[27] Agnihotri, V., Sabharwal, M., Goyal, V.: The extraction of key distinct features for identification and classification of helicopters using micro-doppler signatures. In: IEEE International Conference on Dependable, Autonomic and Secure Computing (DASC/PiCom/CBDCom/CyberSciTech), Fukuoka, Japan, pp. 893–896 (2019). https://doi.org/10.1109/DASC/PiCom/CBDCom/CyberSciTech.2019.00164